Temporal Analysis of Temperature Distribution at a Laser Spot in Selective Laser Thermoregulation Using a High-Speed Radiation Thermometer

Shuta Kanai[1], Tomomasa Ohkubo[*1], Shota Ui[1], Yusaku Kawarazaki[1], Ei-ichi Matsunaga[1], Ken Goto[2], and Yutaka Kagawa[1]

[1]*Tokyo University of Technology, Japan*
[2]*Institute of Space and Astronautical Science, Japan Aerospace Exploration Agency, Japan*
[*]*Corresponding author's e-mail: ookubotmms@stf.teu.ac.jp*

To clarify the mechanical properties of new high heat-resistant materials, the Selective Laser Thermoregulation (SLT) method, a method of accelerated heating tests using a high-power laser, is being developed. The SLT method uses a galvano scanner to scan the surface of the area to be heated with a fiber laser, aiming to heat the sample while dynamically compensating the temperature distribution. However, the SLT method has a problem: the sample's temperature distribution fluctuates spatially and temporally due to the movement of the irradiation point of the laser, which heats the target to a high temperature. In this study, a 400 W fiber laser was scanned back and forth over the sample at scan speeds of 5, 10, and 15 m/s, respectively, and the sample temperature distribution was measured using a high-speed radiation thermometer at 1000 fps. The temperature distribution of the sample was measured using a high-speed radiation thermometer at 1000 fps. The amount of temperature increase at the laser spot was evaluated by curve fitting. The temperature increases at the laser spot decreased to 95.0, 85.1, and 75.7 K when the scan speeds were increased to 5, 10, and 15 m/s, respectively. For all scan speeds, the temperature increase at the laser spot was smaller at locations where the sample temperature was higher. The local temperature increase at the laser spot was successfully suppressed to about 4.5% of the maximum temperature of the entire sample without the laser spot.
DOI: 10.2961/jlmn.2024.02.2008
Keywords: Selective Laser Thermoregulation (SLT) system, laser heating test, galvano scanner, fiber laser, high heat-resistant materials

1. Introduction

In modern society, there are many situations where high heat-resistant materials are required, such as in aircraft engines, blast furnaces, and nuclear reactors. Various high heat-resistant materials have been proposed for these applications. Conventional heating test methods for high heat-resistant materials use furnaces. However, this method has a disadvantage: it takes time to heat and cool the furnace. Therefore, a heating test method using a high-power laser has been proposed as a technique to heat samples in a short time. For example, an accelerated heating test using a CO_2 laser was reported by Appleby et al. in 2015 [1], and an accelerated heating test using a fiber laser was reported by Whitlow et al. in 2019 [2]. These previous studies targeted SiC/SiC Ceramic Matrix Composites, which are expected to be used as turbine materials in next-generation aircraft engines [3][4]. However, both previous studies used a method in which a shaped laser is irradiated to the sample at a fixed point for heating. With these methods, it is difficult to form a uniform temperature distribution on the heated surface of the sample because it is difficult to dynamically compensate for changes in the temperature distribution due to heat transfer and heat conduction.

Therefore, we have developed the Selective Laser Thermoregulation (SLT) method to dynamically compensate the temperature distribution in the evaluation area by moving the laser spot[5]. The SLT method uses a fiber laser and a galvano scanner to scan the surface of the area to be heated with a laser spot, which heats the sample like a coloring book. This method aims to achieve temperature compensation by scanning the laser repeatedly to paint, for example, an area where the temperature has decreased. However, the SLT method has the problem that the sample's temperature distribution fluctuates spatially and temporally because the position of the laser spot where the temperature rise occurs is always moving. In the case of laser processing such as laser welding, it is desirable that the temperature rise at the spot be localized, but in the SLT method, a localized temperature rise at the laser spot is undesirable for forming a stationary temperature distribution. Therefore, it is necessary to find the laser irradiation conditions that provide uniformity of the temperature distribution and temporal stability.

There are many parameters that determine the laser irradiation conditions, and since the SLT method is different from conventional laser processing, there is no accumulated know-how. Therefore, the development of AI to estimate the laser irradiation conditions that reproduce the required temperature distribution is underway [6][7]. However, current

AI can estimate the laser irradiation conditions when the laser is irradiated at a fixed point, but it cannot estimate the conditions under which the laser is scanned.

In this study, the temperature distribution of a sample actually heated by the SLT method was measured with a high-speed radiation thermometer. The high-speed thermometer enabled the tracking of the laser's movement and clarified the relationship between the laser spot's movement and the temperature rise. The temperature increase at the laser spot was quantitatively evaluated by a curve fitting the obtained temperature distribution. The amount of temperature increase at the laser spot was then determined by varying the laser scan speed and sample temperature.

2. Experimental Method

A proportional test piece No. 14B (JIS z2241), shown in Fig. 1, was used as the sample. The material is SUS304, the thickness of the sample is 3 mm, the total length is 120 mm, and the evaluation area is 30 mm at the center of the sample with a width of 8 mm.

A conceptual diagram of the experimental setup is shown in Fig. 2. A fiber laser (Model number: FEC4000M) was used to heat the sample. The diameter of the optical fiber is 0.08 mm, and the focal length of the optical lens is 700 mm. The spot diameter on the specimen was 7.5 mm, and the laser was irradiated at a power of 400 W. The laser was moved by a galvano scanner along the centerline of the sample in the x-axis direction, repeatedly moving back and forth within a range of 100 mm. The laser scan speed was varied from 5, 10, and 15 m/s, and two experiments were conducted at each scan speed.

The temperature distribution on the heated surface of the specimen was measured by a high-speed radiation thermometer at a frame rate of 1000 fps. We used an infrared camera for laser applications (model number: PI08M) made and calibrated by Optris GmbH for measuring temperature distribution.

The sample was heated until it reached a quasi-steady state in which the maximum temperature fluctuation in the evaluation area was constant, and the measurement results were evaluated.

3. Curve fitting method

In this study, the two-dimensional temperature distribution of the sample was measured by a radiation thermometer, as shown in Fig. 3. We focused on the temperature distribution on the center line of the sample in the x-axis direction, as shown in the graph in Figure 3. As shown in Fig. 4, the temperature distribution is considered to have a Gaussian shape for the laser spot and a quadratic shape for the entire sample except for the laser spot. In order to quantitatively evaluate the position of the laser spot and the amount of temperature increase, the measured temperature distribution was curve-fitted using the following equation (1). The definitions of each parameter used in Equation (1) are shown in Table 2.

$$T = q(x - x_b)^2 + T_b + \Delta T_s \exp\left(\frac{2(x - x_s)^2}{r_s^2}\right) \quad (1)$$

For curve fitting, 100 data frames were used after the sample temperature had reached a quasi-steady state. The gripping area, which grips both ends of the specimen, is cooled by water so that the temperature of the specimen decreases towards the two ends. Therefore, the temperature of the specimen falls below the measuring instrument's measuring temperature except near the specimen's center. For this reason, the curve fitting area was 30 mm at the center of the sample. The frames with $\Delta T_s > 0$ in the curve fitting results were defined as the frames with the laser spot in the evaluation area. The magnitude of ΔT_s for frames with a laser spot within the range of $|x_s| < 30$ mm, where the presence of a laser spot can be accurately determined, was also evaluated.

4. Results

The time variation of the maximum temperature in the evaluation region at a scan speed of 15 m/s is shown in Fig. 5, and Fig. 6 shows examples of the temperature distribution in four scenes with different laser spot positions. As shown in Fig. 5, the maximum temperature in the evaluation region oscillates between 1350 K and 1430 K in the quasi-steady state. This temperature difference is roughly consistent with the temperature difference between the maximum temperature of 1410 K when the laser spot is in the center and the maximum temperature of 1360 K when the laser spot is not present, as shown in Fig. 6. The temperature distribution in the heated region is similar to that shown in Fig. 4, as shown in Fig. 6.

Table 1 Definition of curve fitting parameters.

q []	Coefficient of the second order of the overall temperature distribution
x_b [m]	Center of the overall temperature distribution
T_b [K]	Temperature of the overall temperature distribution at x_b
x_s [m]	Center of the laser spot
T_{sb} [K]	Temperature of the overall temperature distribution at x_s
ΔT_s [K]	Spot temperature rise: $T(x_s) - T_{sb}$
r_s [m]	Laser spot radius

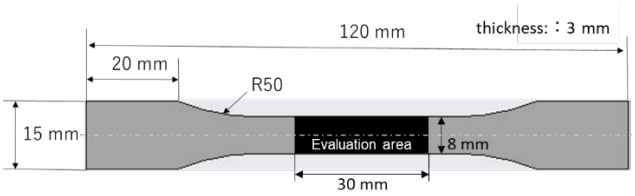

Fig. 1 Sample shape.

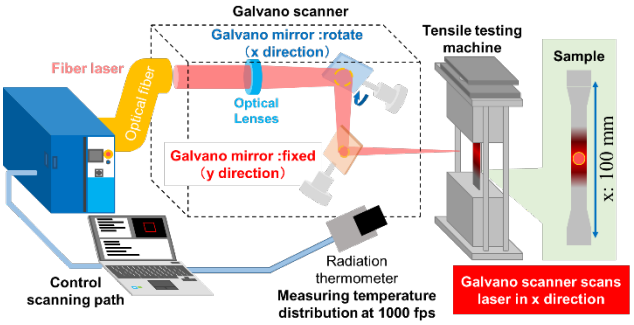

Fig. 2 Experimental setup.

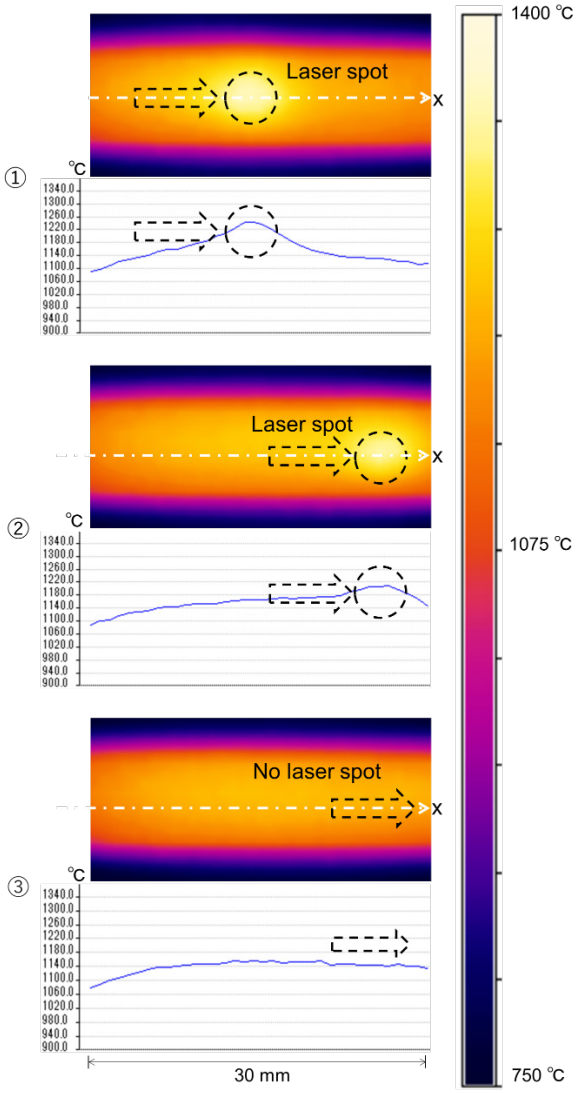

Fig. 3 Example of temperature distributions for three consecutive frames. The one-dimensional graphs are the temperature distributions on the respective white single-dashed lines.

The time averages of ΔT_s at each scanning speed obtained by curve fitting are shown as dots, and the standard deviations over time are shown as error bars in Fig. 7. In the following graphs, the first experiment at each scanning speed is denoted by ①, and the second experiment by ②. At scan speeds of 5, 10, and 15 m/s, the time averages of ΔT_s were 95.0, 85.1, and 75.7 K for the first experiment and 103.6, 73.6, and 61.3 K for the second experiment, respectively. The standard deviations of ΔT_s over time were 17.5, 24.6, and 27.6 K in the first experiment and 18.3, 18.7, and 15.2 K in the second experiment. These results show that the time average of ΔT_s becomes smaller as the scanning speed increases. On the other hand, there was no significant change in the standard deviation of ΔT_s.

Next, Fig. 8 shows the relationship between ΔT_s and T_{sb} for each scan speed. The ΔT_s was also smaller as the sample temperature T_{sb} increased for all scan speeds.

5. Discussion

The time average of ΔT_s at a scan speed of 5 m/s is 103.6 K. This is about 7.2% of the average value of T_b of 1433 K for the same scan speed. In contrast, the time average of ΔT_s at a scan speed of 15 m/s is 61.3 K, which is about 4.5% of the average T_b value of 1365 K for the same scan speed. This suggests that a faster scan speed can reduce the ratio of the temperature increase of the laser spot to the overall temperature.

If the scanning speed is fast enough, the temperature rise at the laser spot is expected to occur in a short time. Therefore, a simple physical model that considers only heating by the laser and cooling by radiation is used here to discuss qualitatively ΔT_s. The definitions of the parameters used in the discussion are summarized in Table 2. The amount of increase in internal energy in the region measured by each pixel of the radiation thermometer is determined by the heating energy provided at the moment the laser spot is passed by the laser and the cooling energy provided by radiation. Considering this energy balance, ΔT_s can be expressed by the following equation (2). In other words, to reduce ΔT_s, it is effective to increase the scan speed v and the temperature T_{sb} at the spot, excluding the temperature increase due to the spot.

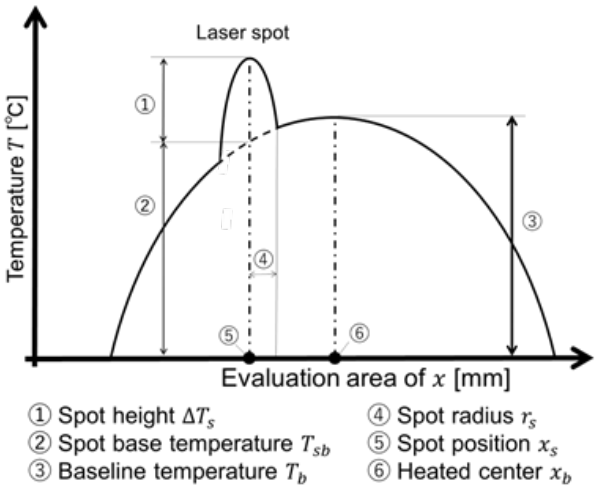

Fig. 4 Definition of fitting parameters.

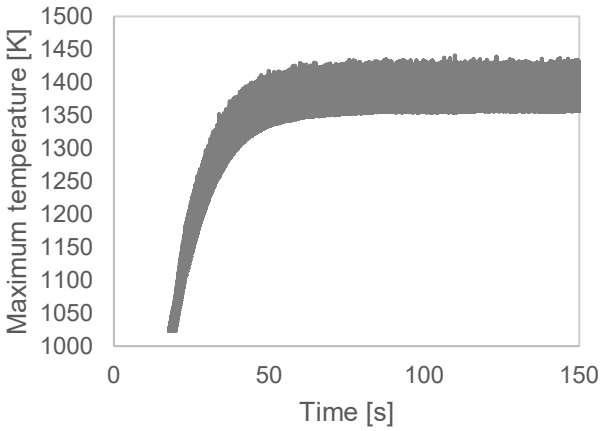

Fig. 5 Time variation of maximum temperature (15 m/s) .

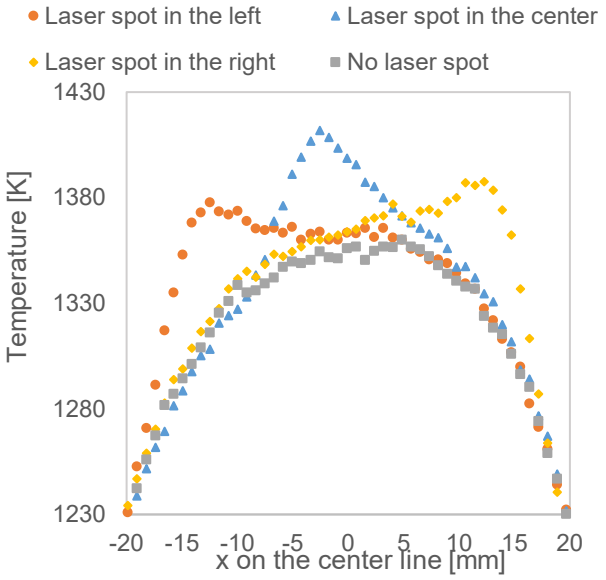

Fig. 6 Example of temperature distribution (15 m/s) .

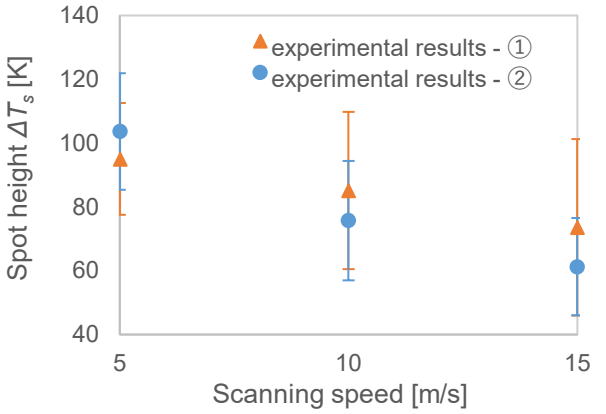

Fig. 7 Time average of spot height.

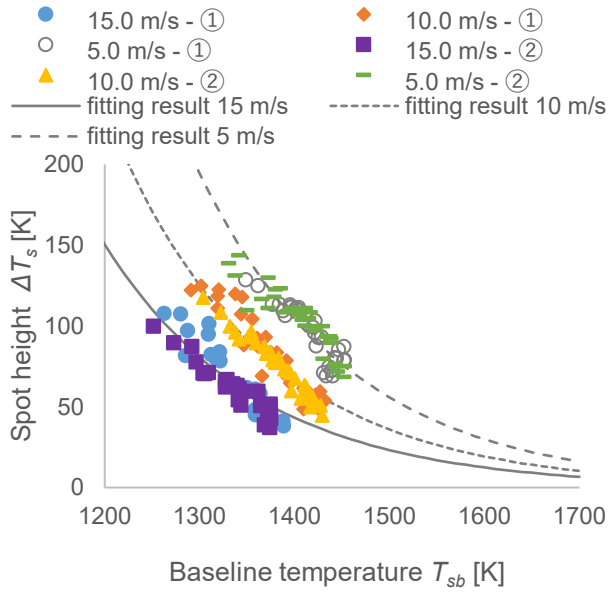

Fig. 8 Variation of spot height with sample temperature.

Table 2 Definition of physical model parameters.

$\boldsymbol{v}$ [m/s]	Laser scanning speed
$\boldsymbol{L}$ [m]	Length per pixel of the image taken by the radiation thermometer
$\boldsymbol{I_{laser}}$ [W/m^2]	Intensity at the center of the laser
$\boldsymbol{\varepsilon_{laser}}$	Absorption rate of the laser
$\boldsymbol{\varepsilon_{rad}}$	Emissivity
$\boldsymbol{\sigma}$ [W /m^2/K^4]	Stefan-Boltzmann constant
$\boldsymbol{T_0}$ [K]	Atmosphere temperature
$\boldsymbol{\rho}$ [kg/m^3]	Density of the sample
$\boldsymbol{C}$ [J/kg/K]	Specific heat of the sample
$\boldsymbol{d}$ [m]	Laser absorbing thickness

$$\Delta T_s = \frac{\frac{L}{v}\left(\varepsilon_{\text{laser}} I_{\text{laser}} - \varepsilon_{rad}\sigma(T_{sb}^4 - T_0^4)\right)}{\rho C d} \quad (2)$$

To discuss ΔT_s for larger T_{sb} from the experimental results shown in Fig. 8, we performed curve fitting using equations (3) and (4), expressed in terms of scan speed v and T_b.

$$\Delta T_s = a\exp(bT_{sb}) \quad (3)$$
$$a = \alpha\exp(\beta v) \quad (4)$$

First, the results shown in Fig. 8 for each scan speed were curve-fitted using Equation (3) to obtain the values of a and b. Next, b was fixed to -0.00624, the average of all curve-fitting results using Equation (3). Next, b was fixed at -0.00624, which is the average of all curves fitting results using Equation (3), and the results for each scan speed were again fitted using Equation (3) to obtain the value of a. The obtained value of a was then fitted using Equation (4). As a result, ΔT_s was expressed as v and T_{sb} in Equation (5).

$$\Delta T_s = 1009944\exp(-0.0882v)\exp(-0.00624T_{sb}) \quad (5)$$

The curves shown in Fig. 8 are the results of fitting the experimental results at each scan speed using Equation (5).

Considering the case where the sample is heated up to 1700 K, which is the expected operating temperature of SiC/SiC CMC, ΔT_s are 16, 10, and 7 K at scan speeds of 5, 10, and 15 m/s, respectively, as shown in the curve in Fig. 8. These ΔT_s are less than 1 % of 1700 K. This means that if the temperature of the sample can be heated up to about 1700 K, even if the scan speed is slowed down to about 5 m/s for temperature compensation, heating at the laser spot is not expected to be a problem.

6. Conclusion

We quantitatively evaluated the change in the temperature rise of the laser spot by using curve fitting when the scan speed of the laser is changed in the SLT method.

It was found that the temperature increase at the laser spot became smaller as the scan speed was increased. In particular, when the scan speed was 15 m/s, the temperature increase at the laser spot was successfully suppressed to about 4.5% of the overall maximum temperature.

Qualitative discussions revealed that increasing the temperature of the sample increases the influence of radiation, resulting in a smaller temperature increase at the laser spot. This suggests that the temperature rise at the laser spot can

be suppressed to less than 1% of the total temperature if the sample is heated to about 1700 K, which is the melting point of SUS304.

The knowledge of local changes in the temperature distribution during high-speed laser scanning obtained in this study is expected to lead to highly accurate control of the heating distribution by the SLT method. Furthermore, it is also expected to advance other techniques for scanning lasers at high speed, such as wabbling in laser welding.

In the future, we aim to perform heating tests on various high heat-resistant materials, such as SiC/SiC CMCs.

References

[1] M.P. Appleby, D. Zhu, and G. Morscher: surf Coat technol, 284, (2015) 318.
[2] T. Whitlow, J. Pitz, J. Pierce, S. Hawkins, A. Samuel, K. Kollins, G. Jefferson, E. Jones, J. Vernon, and C. Przybyla: Composite Structures, 210, (2019) 179.
[3] G.S. Corman and K.L. Luthra: "Handbook of Ceramic Composites" ed. By N. P. Bansal, (Publisher, Boston, 2005) p.99.
[4] M. Roode, J. Price, J. Kimmel, N. Miriyala, D. Leroux, A. Fahme, and K. Smith: J. Eng. Gas Turbines Power, 192, (2007) 21.
[5] H. Koshiji, T. Ohkubo, K. Azato, Y. Kameda, E. Matsunaga, T. Dobashi, N. Shichijo, K. Goto, M. Sato, C. Fujiwara, and Y. Kagawa: J. Laser Micro Nanoeng., 15, (2020), 174.
[6] M. Nakaone, T. Ohkubo, Y. Ueno, K. Goto, and Y. Kagawa: J. Laser Micro Nanoeng., 16, (2021), 84.
[7] M. Nakaone, T. Ohkubo, Y. Ueno, K. Goto and Y. Kagawa: J. Laser Micro Nanoeng., 17, (2022) 194.

(Received: June 9, 2024, Accepted: September 15, 2024)